HHS Public Access

Author manuscript

Circulation. Author manuscript; available in PMC 2019 August 28.

Published in final edited form as:

Circulation. 2018 August 28; 138(9): 913–928. doi:10.1161/CIRCULATIONAHA.118.033939.

TBX20 Regulates Angiogenesis through the PROK2-PROKR1 Pathway

Shu Meng, MD, PhD[1,*], **Qilin Gu, PhD**[1,*], **Xiaojie Yang, PhD**[1], **Jie Lv, PhD**[1], **Iris Owusu, MS**[1], **Gianfranco Matrone, PhD**[1], **Kaifu Chen, PhD**[1], **John P. Cooke, MD, PhD**[1,¶], and **Longhou Fang, PhD**[1,¶]

[1]Center for Cardiovascular Regeneration, Department of Cardiovascular Sciences, Houston Methodist Research Institute, 6670 Bertner Avenue, R10-South, Houston, TX 77030

Abstract

Background—Angiogenesis is integral for embryogenesis, and targeting angiogenesis improves the outcome of many pathological conditions in patients. TBX20 is a crucial transcription factor for embryonic development, and its deficiency is associated with congenital heart disease. However, the role of TBX20 in angiogenesis has not been described.

Methods—Loss- and gain-of-function approaches were used to explore the role of TBX20 in angiogenesis both *in vitro* and *in vivo*. Angiogenesis gene array was used to identify key downstream targets of TBX20.

Results—Unbiased gene array survey showed that *TBX20* knockdown profoundly reduced angiogenesis-associated *PROK2* gene expression. Indeed, loss of TBX20 hindered endothelial cell migration and *in vitro* angiogenesis. In a murine angiogenesis model using subcutaneously implanted matrigel plugs, we observed that TBX20 deficiency markedly reduced PROK2 expression and restricted intra-plug angiogenesis. Furthermore, recombinant PROK2 administration enhanced angiogenesis and blood flow recovery in murine hindlimb ischemia. In zebrafish, transient knockdown of *tbx20* by morpholino antisense oligos (MO) or genetic disruption of *tbx20* by CRISPR/Cas9 impaired angiogenesis. Furthermore, loss of *prok2* or its cognate receptor *prokr1a* also limited angiogenesis. In contrast, overexpression of *prok2* or *prokr1a* rescued the impaired angiogenesis in *tbx20* deficient animals.

Conclusions—Our study identifies TBX20 as a novel transcription factor regulating angiogenesis through the PROK2-PROKR1 pathway in both development and disease, and reveals a novel mode of angiogenic regulation whereby the TBX20-PROK2-PROKR1 signaling cascade may act as a “biological capacitor” to relay and sustain the pro-angiogenic effect of VEGF. This pathway may be a therapeutic target in the treatment of diseases with dysregulated angiogenesis.

Correspondence to: John P. Cooke, M.D., Ph.D., Chair, Department of Cardiovascular Sciences, Houston Methodist Research Institute, 6670 Bertner Ave., Mail Stop: R10-South, Houston, Texas, 77030, Phone: 713-441-8322, Fax: 713-441-7196, jpcooke@houstonmethodist.org. Longhou Fang, PhD, Department of Cardiovascular Sciences, Houston Methodist Research Institute, 6670 Bertner Ave., Mail Stop: R10-South, Houston, Texas, 77030, Phone: 713-363-9012, Fax: 713-441-7196, lhfang@houstonmethodist.org.

*contributed equally

¶co-corresponding authors

Disclosures

None.

Keywords

Angiogenesis; TBX20-PROK2-PROKR1 signaling axis; G protein coupled receptor; PAD; Proangiogenic capacitor

Introduction

T-box 20 (*TBX20*) encodes a key transcription factor (TF) that is expressed in the heart, eyes, ventral neural tube, and limbs during embryonic development[1]. It belongs to the phylogenetically conserved family of T-box genes that share a common T-box DNA-binding domain. In zebrafish, *tbx20* is expressed in the developing heart and dorsal aorta[2, 3], and regulates cardiac development[4]. *Tbx20* knockout in mice causes a variety of cardiac defects and results in embryonic lethality around E10.5[5–7]. In humans, mutations in *TBX20* are associated with a complex spectrum of developmental abnormalities, including defects in septation, chamber growth, valvulogenesis and cardiomyopathy[8].

TBX20 regulates endocardial cushion cell proliferation, extracellular matrix gene expression and septation[9, 10], in part via modulation of Lef1 and the Wnt/β-catenin pathway[11]. In addition, TBX20 promotes heart chamber formation in part through repression of TBX2[5–7]. Whereas a partial deficiency of TBX20 may cause congenital heart defects, a greater deficiency of TBX20 hinders motoneuron development[12].

Tbx20 is also expressed in the adult heart, where overexpression of *Tbx20* in adult cardiomyocytes promotes proliferation[13, 14] and improves myocardial infarction outcomes in mouse model[13, 15]. In endothelial cells (ECs), TBX20 upregulates PPAR-γ and suppresses the generation of reactive oxygen species and the expression of adhesion molecules generated in response to oxidized low-density lipoproteins[16]. However, it is unknown whether TBX20 is involved in blood vessel formation and controls angiogenic processes.

The chimeric heterokaryon model was first used to identify novel genes in nuclear reprogramming to pluripotency[17]. We have adopted the model to identify novel genes in endothelial development[18]. In this model, murine embryonic stem cells (ESCs) are fused with adult human ECs, and RNA-seq is performed at intervals to assess changes in global gene expression of the resulting hybrid cells. We found that factors maintaining endothelial phenotype act on the ESCs to induce the expression of genes associated with endothelial lineage[18]. Using this model, we discovered novel genes implicated in endothelial development. TBX20 was upregulated early after cell fusion in this chimeric heterokaryon model, which prompted us to explore the role of TBX20 in endothelial development. Our subsequent work illuminates a new TBX20-choreographed molecular pathway for developmental and pathological angiogenesis.

Methods

The data, analytic methods, and study materials will be made available to other researchers for purposes of reproducing the results or replicating the procedure upon request.

Animal husbandry

All animals were maintained in a specific pathogen-free facility at Houston Methodist Research Institute in Houston. Animal use and care were approved by the Houston Methodist Animal Care Committee in accordance with institutional animal care and use guidelines. NOD-SCID mice were generated in our laboratory. Zebrafish AB wild type, mutant and *Tg(fli1:EGFP)*^{y1} fish lines were maintained and bred as described previously[19, 20].

Matrigel plug assay

To assess the role of Tbx20 in angiogenesis *in vivo*, matrigel was mixed with 50 ng/ml VEGF, 30 U/ml heparin to stabilize VEGF[21], and with 2 μM scramble siRNA or siRNA targeting *Tbx20* in a final volume of 400 μL and injected subcutaneously into the lower abdominal region of SCID mice. After five days, the matrigel plugs were removed for FACS analysis, RNA extraction or histology analysis. The investigator who analyzed the matrigel plugs was blinded to the initial treatment.

Murine hindlimb ischemia

Hindlimb ischemia was induced in 9-month old male wild type mice as previously reported with slight modification[21–23]. Briefly, unilateral hindlimb ischemia was induced by ligating the femoral artery and its major branches. Afterwards, the mice were housed individually and blood flow in the affected and control limbs was imaged up to 21 days. In some experiments, recombinant PROK2 proteins (0.1 μg/g body weight) or PBS was injected i.m. immediately and 7 days after surgery. Blood perfusion was monitored before and immediately after surgery, and 4, 7, 11 and 14 days post-operatively. The clinical ischemia score index was used to assess tissue loss, as modified from the previously reported method[24]. The criteria used were: 0 - No changes; 1 - Discoloration/Necrosis of the nails; 2 - Discoloration/Necrosis of the toes; 3 - Foot Necrosis; 4 - Leg Necrosis (up to the gastrocnemius muscle); 5 - Autoamputation (loss of limb). There were two independent observers, blinded to the group assignment. At day 14 in the postoperative period, the hindlimb muscles from the operated and contralateral limbs collected for histology. Eight male mice were used for each experimental group. Total capillary density of the ischemic hindlimb cross sections was determined by staining the slides with rabbit anti-mouse CD31 (BD Biosciences), followed by horseradish peroxidase–conjugated secondary antibody.

Laser Doppler based tissue perfusion measurement

Blood flow to the ischemic or non-operated (nonischemic) hindlimb was assessed using a PeriScan PIM3 laser Doppler system (Perimed AB, Sweden) as described previously[22, 23]. Animals were prewarmed to a core temperature of 37.5 °C and heart rate was constantly monitored for signs of stress from overheating. Hindlimb blood flow was measured pre- and postoperatively on selected days (0, 4, 7, 11 and 14). Blood perfusion rate was measured via laser Doppler scans. The level of perfusion in the ischemic and unoperated hindlimbs was quantified using the mean pixel value within the region of interest, and the relative changes in hindlimb blood flow were expressed as the ratio of the left (ischemic) over right (unoperated) Laser Doppler-detected blood perfusion.

Generation of zebrafish mutants using CRISPR/Cas9

The CRISPR/Cas9-mediated gene knockout technology in wild type AB line zebrafish was performed as previously described[25]. In brief, the target sequences for *tbx20*, *prok2* and *prokr1a* were 5′-TGTGCTAATGGACATAGTTC-3′, 5′-GGATGCACATTCGGAGACTG-3′ and 5′-GGCAATATCAGACTTTCTGG-3′, respectively. Complementary target oligonucleotides were annealed and inserted into pT7-gRNA vector. Guide-RNA (gRNA) was synthesized using HiScribe T7 Quick High Yield RNA Synthesis kit. The pCS2-nCas9n was linearized using NotI and capped Cas9 mRNA was synthesized using mMESSAGE mMACHINE SP6 kit. The gRNA (50–100 ng/μl) and Cas9 mRNA (150–200 ng/μl) was mixed and injected into one-cell stage WT AB embryos.

For detecting the zebrafish mutants, genomic DNA was extracted from individual zebrafish larva and a short genomic region (300–500 bp) flanking the target site was PCR amplified. Purified PCR products (200 ng) were denatured and reannealed, and then digested with T7 Endonuclease I (NEB). PCR products of positive mutants were subcloned into pMD20-TA vector (Clontech). After transformation into competent cells and overnight culture at 37°C, single colony was selected for sequencing.

RNA extraction and Quantitative Real-Time PCR (qRT-PCR)

qRT-PCR in zebrafish and mice was performed as previously described[19, 26–28]. Primers used in zebrafish study were list in Table S1. Please see supplementary materials for details.

Whole-mount alkaline phosphatase staining

Zebrafish embryos were fixed in 4% paraformaldehyde (PFA) at 3 days post-fertilization and stained for endogenous alkaline phosphatase activity similar to previously described[29, 30]. Briefly, the embryos were fixed in 4% PFA overnight at room temperature, and were serially dehydrated and permeabilized in 25%, 50%, 75% methanol in PBST (phosphate buffered saline with 0.1% Tween-20, pH 5.5) (v/v), and 100% methanol, following by rehydrated in 75%, 50% and 25% methanol and finally in PBST. After equilibrated with alkaline phosphatase buffer, the embryos were stained using the NBT/BCIP solution at room temperature for 20 minutes. The reaction was stopped with stop buffer (PBST with 0.25 mM EDTA, pH 2.2). Embryos were mounted in glycerol for image capture.

Confocal imaging and data analysis

Anaesthetized embryos at indicated stage were mounted in 1.0% low-melt agarose (Sigma Aldrich) for imaging[19]. Images were acquired by using an Olympus FluoView FV1000 laser scanning confocal microscope. Z-stacks were acquired with a 3 μM z-step, and images were 3D rendered. Neurolucida software (MBF Bioscience) was used to analyze the length of ISVs and SIV.

Data analysis

Results were expressed as mean±SEM, and statistical analysis was performed using Student's *t*-test, one-way or two-way analysis of variance (ANOVA) followed by Sidak's

multiple comparisons test using Prism software. *p<0.05 was considered statistically significant. **, p ≤ 0.01, ***, p ≤ 0.001, ****, p ≤ 0.0001.

Results

Tbx20 is robustly upregulated in a heterokaryon model

To examine the *Tbx20* gene expression in endothelial differentiation, two model systems were used, one is the mESC differentiation to ECs and the other one is heterokaryon induced differentiation of pluripotent stem cells into endothelial lineage. During the mESC differentiation into endothelial lineage[18], *Tbx20* gene expression was upregulated by 16-fold at day 8 of differentiation compared with mESCs (Fig. S1a). In a heterokaryon model[18], fusing mESC with HUVECs induced differentiation of pluripotent stem cells toward endothelial lineage. We found that *Tbx20* gene expression was upregulated and peaked at 4-fold at 6 hours after heterokaryon formation compared with co-culture control (CT, Fig. S1b).

Tbx20 is essential for developmental angiogenesis in zebrafish

Based on our findings from the heterokaryon model, we hypothesized that *TBX20* transcriptionally regulates vascular development. Accordingly, we first knocked down *tbx20* in zebrafish embryos by injecting *tbx20* MO at the one-cell stage embryo of *Tg(fli1:EGFP)*^{y1} zebrafish. These animals express enhanced green fluorescent protein (EGFP) in the endothelium[31], permitting visualization of vascular development in both trunk and yolk sac regions. At 30 hours post-fertilization (hpf), the *tbx20* knockdown (KD) embryos, compared to controls, showed no apparent change in vasculogenesis as evidenced by normal dorsal aorta and cardinal vein formation (Fig. 1a). At this time point, intersegmental vessels (ISVs), which sprout from dorsal aorta via angiogenesis including endothelial proliferation and migration[32], reached the dorsal roof of the neural tube in control embryos (Fig. 1a, 1c and Fig. S1c). In contrast, ISVs sprouted only halfway through their dorsal trajectory and stalled at the boundary between the notochord and neural tube in *tbx20* morphants (Fig. 1a, 1c and Fig. S1c). In addition, *tbx20* deficiency suppressed the development of subintestinal vessels (SIVs), which form bilaterally over the dorsal-lateral aspect of the zebrafish yolk at 3 day post-fertilization (dpf), in the shape of a basket that extends from the ventral edge of the somite[33] (Fig. 1b, 1c and Fig. S1d). Coinjection of the zebrafish *tbx20* mRNA, which lacked the MO targeting site, significantly rescued the ISV and SIV defects in *tbx20* morphants (Fig. 1a–c, Fig. S1c & d). All the above data suggest that *tbx20* is required for developmental angiogenesis.

Since MO-mediated transient gene KD could have off-target effects[34], we also generated *tbx20* knockout (KO) mutants to further validate the MO-induced vascular defects. We generated the *tbx20* KO zebrafish mutants using CRISPR/Cas9 to target the third exon of *tbx20* (Fig. 1d). Zebrafish full-length *tbx20* encodes a protein of 446 amino acid (AA). The *tbx20* mutants had a 4-bp deletion starting at the 453 nucleic acid position (Fig. 1e), resulting in frameshift and a premature stop codon encoding a truncated protein of only 193 AA (Fig. 1f). This mutation disrupted the original T-box domain (98–290 AA) and the DNA binding domain[35], designed to abolish its transcriptional activity.

Blood vessels in *tbx20* mutants showed incomplete vessel length, attenuated sprouting of SIVs and reduced vascular area compared with controls (Fig. 1g & h) as examined using whole-mount staining for endogenous alkaline phosphatase activity[30]. These phenotypes are congruent with *tbx20* morphants, suggesting that the angiogenic phenotype of *tbx20* morphant was not due to MO off-target effects, and that *tbx20* regulates *in vivo* vascular development in zebrafish. Previous studies found that constitutive KO mutations, but not transient KD, may activate compensatory mechanisms[36] and thus cause discrepancies in the observed phenotype between KD and KO animals. However, we observed impaired developmental angiogenesis in both *tbx20* KD and KO, suggesting that *tbx20* plays a critical role in developmental angiogenesis, uncompensated by other mechanisms.

ISV angiogenic sprouts originate at about 20 hpf from the dorsal aorta, which condenses as a distinct cord of ECs at the trunk midline starting at the 15 somite stage (16.5 hpf)[32]. Since *tbx20* is reported to regulate heart development, we next examined whether the impaired angiogenesis is secondary to a defect of heart development and associated hemodynamic perturbations. We used the pan-cardiac marker, *cardiac-myosin light chain-2* (*cmlc2*), to examine the formation of arterial precursors as reported[37]. At 24 hpf, *cmlc2* expression in *tbx20* morphants were comparable to that in control animals, suggesting that the specification of arterial precursors proceeds normally in *tbx20*-MO injected animals. At 30 hpf, we did not observed abnormal heart development in low dose *tbx20* MO injected animals (Fig. S2 and Table S2), which agreed with previous report that *tbx20* is not essential for the early (up to 24 hpf) differentiation or morphogenesis of the heart[4]. Altogether, these data indicate that the impaired angiogenesis in Tbx20-deficient animals is not an indirect effect of disturbed hemodynamics caused by dysregulated heart development.

Tbx20 is required for pathological angiogenesis in mice

To determine if *Tbx20* has a role in pathological angiogenesis in adult animals, we prepared matrigel that was mixed with *Tbx20* siRNA or scrambled control siRNA, and injected the matrigel subcutaneously into NOD-SCID mice. The matrigel is in a liquid form at 4 °C, and condenses into a solid plug when injected into mice. This model is widely used to assess angiogenesis. Our data demonstrated that matrigel plugs containing the scrambled siRNA showed robust angiogenic response, and were imbued with vessels containing red blood cells as evidenced by bright field imaging and by HE staining (Fig. 2a & b). By contrast, intra-plug vessels and blood content was markedly reduced in those plugs containing *Tbx20* siRNA (Fig. 2a & b). FACS analysis of the cell content in matrigel plugs revealed a decrease in $CD144^+$ ECs (Fig. 2c & d) from *Tbx20* siRNA-containing matrigel plugs (0.41% vs 4.96% in CT). We verified successful KD of *Tbx20* gene expression in the matrigel plug using qRT-PCR (Fig. 2e).

To explore the role of *TBX20* in angiogenesis *in vitro*, we knocked down *TBX20* in human umbilical vein ECs (HUVECs) and examined the effect on tube formation, migration and proliferation. We generated a stable *TBX20* KD line and CT HUVECs using lentiviral vector-mediated delivery of shRNA against *TBX20* or scrambled CT shRNA. Compared with CT cells, qRT-PCR analysis showed a 50% decrease in *TBX20* gene expression (Fig. 2f), and western blot analysis revealed a 60% reduction in protein levels (Fig. 2g) in the

TBX20 KD cells. *TBX20* KD HUVECs maintained the normal cobblestone morphology compared with CT cells (Fig. S3a).

Since angiogenesis consists of endothelial migration and proliferation, we examined these functions in *TBX20* KD cells. The *TBX20* KD did not significantly reduce cell proliferation rate (Fig. S3b) albeit slightly reducing the cell fraction in G2/M phase (Fig. S3c & d). *TBX20* KD did not alter acLDL uptake (Fig. S3e & f), the synthesis of NO (Fig. S3g), and the expression of CD31 and CD144 (Fig. S3h–j), compared with CT cells. However, *TBX20* KD markedly impaired VEGF-induced tube formation (Fig. 2h), and suppressed cell migration in a scratch assay (Fig. 2i & j) Altogether, these data suggest that *TBX20* regulates angiogenesis mainly through EC migration.

Prokineticin 2 (PROK2) mediates the effect of TBX20

To identify downstream molecules of *TBX20* in angiogenesis, we examined the gene expression of 84 angiogenesis-related genes using a Qiagen Angiogenesis RT Profiler PCR Array. Sixteen genes were downregulated over 2-fold in the *TBX20* KD HUVECs compared with CT (Fig. 3a). Among them, *PROK2* was downregulated over 12 fold, one of the most pronouncedly responsive genes in *TBX20* KD cells.

PROK2 is a secreted protein and is known to have diverse functions in angiogenesis[38, 39], behavioral circadian rhythm[40], olfactory bulb morphogenesis[41] and reproductive function[42]. In adult zebrafish, *prok2* is involved in both constitutive and injury-induced neurogenesis[43]. To examine whether *PROK2* mediated the impaired angiogenic processes in *TBX20* KD cells, we determined the rescue effect of PROK2 on the defective network formation in TBX20-deficient HUVECs. As expected, supplementation with exogenous PROK2 restored normal tube formation in *TBX20* KD HUVECs (Fig. 3b).

In addition, we generated *TBX20* overexpression (OE) HUVECs and examined the *PROK2* gene expression. Both qRT-PCR (Fig. 3c) and western blot analysis (Fig. 3d) validated the stable overexpression of *TBX20*. As expected, *TBX20* OE further promoted EC migration (Fig. 3e), and strongly upregulated *PROK2* gene expression (Fig. 3f). Similarly, *Prok2* gene expression was downregulated from matrigel plugs containing *Tbx20* siRNA compared with the ones with CT siRNA (Fig. 3g). Furthermore, knockdown of *tbx20* also diminished *prok2* expression in zebrafish embryo (Fig. 3h). Since VEGF activates the major proangiogenic pathway for angiogenesis, we thus assessed hierarchical relations of VEGF, TBX20 and PROK2 in HUVECs. VEGFA165 stimulation upregulated *TBX20* and *PROK2* gene expression (Fig. 3i & j), an effect that was abolished by TBX20 KD (Fig. 3k & l), suggesting that TBX20 augments VEGF-induced PROK2 gene expression. Although TBX20 knockdown also robustly downregulated FGF1 and FGFR3 expression (Fig. 3a), Fgf1 and Fgfr3 overexpression failed to rescue the angiogenic defects in Tbx20-deficient animals (Fig. S4a & b). Collectively, these results suggest that PROK2 functions downstream of TBX20 in regulating angiogenesis.

Prok2 regulates developmental angiogenesis

We postulate that loss of *prok2* would phenocopy the angiogenesis defects in *tbx20* morphants since Prok2 acts downstream of Tbx20. Indeed, *prok2* KD abolished ISV

formation at 30 hpf (Fig. 4a & c) and SIV development at 3 dpf (Fig. 4b & c), similar to that in *tbx20* morphants. The ISV and SIV defects caused by *prok2* knockdown were largely reversed by the administration of zebrafish *prok2* mRNA that did not include the MO targeting site (Fig. 4a–c, Fig. S5a & b).

We then generated *prok2* KO zebrafish mutants (Fig. 4d–f), which showed abnormal SIV formation with reduced vessel area, decreased SIV length and attenuated sprouting (Fig. 4g & h). Altogether, the *prok2* deficiency phenocopied the *tbx20* deficiency. These findings suggest that Prok2 functions as a key downstream component of Tbx20 in regulating developmental angiogenesis.

PROK2 exerts its angiogenic effects largely through PROKR1

PROK2 signals through two G protein coupled receptors, prokineticin receptor (PROKR) 1[44] and 2[45]. PROKR1 is reported to mediate the pro-angiogenic effect of PROK2 in cardiovascular system[46]. In addition, *PROKR1* overexpression promotes neovascularization[47], while *PROKR2* overexpression induces an inflammatory response[48]. However, the *in vivo* genetic evidence for *PROKR1* in angiogenesis remains unknown.

There is only *prokr1* gene but not *prokr2* gene in zebrafish. Zebrafish has two different *prokr1* genes, *prokr1a* and *prokr1b* that are located on chromosome 1 and 13, respectively. Zebrafish *prokr1a* shares the highest homologue to that of mouse and human *PROKR1*. We thus hypothesized that *prokr1a* encodes the major receptor for Prok2 in zebrafish, and further hypothesized that loss-of-function of *prokr1a* would limit angiogenesis similar to that in *prok2* or *tbx20* deficient animals. Indeed, similar to *tbx20* and *prok2* KD morphants, loss of *prokr1a* resulted in a substantial impairment of ISV formation at 30 hpf and SIV formation at 3 dpf (Fig. 5a). The ISV and SIV defects caused by *prokr1a*-MO were alleviated by the administration of exogenous *prokr1a* mRNA which did not contain the MO binding site (Fig. 5a–c, Fig. S6a & b). We next generated the *prokr1a* knockout zebrafish mutant (Fig. 5d–f). Notably, the *prokr1a* mutants manifested less SIV sprouting than control animals at 3 dpf (Fig. 5g & h). These results suggest that the Prokr1a, a receptor for Prok2, orchestrates angiogenesis in zebrafish.

In HUVECs, both putative PROK2 receptors PROKR1 and PROKR2 can be detected on the cell surface (Fig. 6a). Both PROKR1 and PROKR2 knockdown by siRNA reduced their relative mRNA expression over 70% (Fig. 6b). Interestingly, only PROKR1 knockdown significantly impaired PROK2-mediated angiogenesis (Fig. 6c) and cell migration (Fig. 6d), suggesting that PROK2 controls angiogenesis and EC migration through PROKR1. In addition, PROKR1 KD abolished the PROK2-engaged activation and phosphorylation of ERK1/2 and Akt pathway in HUVECs (Fig. 6e–g). All data indicate that PROKR1 mediates the effect of PROK2 on angiogenesis and endothelial migration.

prok2 or *prokr1a* gene overexpression rescues angiogenesis in *tbx*20 KD animals

Previous studies demonstrate that PROKR1 signaling induces neovascularization[47], whereas PROKR2 signaling governs inflammatory response and impairs endothelial integrity[48]. To further verify that Prokr1 is the major GPCR for Prok2 in angiogenesis, we overexpressed

prokr1a mRNA in *prok2* morphants, and found that forced Prokr1a expression corrected impaired angiogenesis (Fig. 7a & b).

Interestingly, loss of *prok2,* similar to *tbx20* deficiency*,* downregulated *prokr1a* but not *prokr1b* gene expression (Fig. 7c–e), suggesting that Prok2 positively regulates Prokr1a expression during development. We further tested whether *prok2-prokr1a* signaling mediated the effect of Tbx20 on angiogenesis. As expected, injection of *prok2* or *prokr1a* mRNA reversed to a large extent restricted angiogenesis caused by Tbx20 or Prok2 deficiency (Fig. 7a & b). Collectively, these results suggest that Prok2-activated Prokr1a signaling controls angiogenesis downstream of Vegf-induced Tbx20 upregulation.

PROK2 enhances functional recovery from hindlimb ischemia

To examine whether Tbx20-Prok2 pathway is involved in angiogenesis during hindlimb ischemia, we examined the gene expression of *Tbx20*, *Prok2* and *Prokr1* during the recovery following hindlimb ischemia. Intriguingly, both *Tbx20* and *Prok2* gene expression were increased (Fig. 8a & b), but the *Prokr1* gene expression remained stable (Fig. 8c). Notably, *Tbx20* gene expression was upregulated as early as 4 days after ischemia.

Since *Prok2* gene expression was elevated at later time points, we hypothesize that early application of PROK2 will promote angiogenesis and functional recovery from hindlimb ischemia. We injected i.m. recombinant PROK2 protein or vehicle. Notably, we observed increased blood perfusion recovery in the ischemic limb with PROK2 treatment (Fig. 8d & f). In addition, the PROK2-treated mice were improved clinically, as documented by an observer blinded to treatment group using an established clinical scoring system (Fig. 8e). PROK2 administration also increased gastrocnemius capillary density as shown by greater CD31 staining (Fig. 8g). The results suggest that PROK2 treatment enhances functional blood vessel formation following hindlimb ischemia injury.

Discussion

Previous studies showed that the transcriptional factor TBX20 regulates a variety of developmental processes, in particular heart development[4–8]. In this paper, we demonstrate for the first time that TBX20 mediates angiogenic processes *in vitro*; orchestrates vascular development in zebrafish; and modulates the angiogenic response to ischemia in mice. We identified PROK2 as a downstream target for TBX20, and further validated that PROK2-PROKR1 signaling axis mediated the effect of TBX20 on angiogenesis. Thus, our study defined a novel TBX20-regulated signaling pathway for angiogenesis (Fig. S7).

Identification of TBX20 as a novel transcription factor for angiogenesis: selective role in cell migration

We identified TBX20 as a candidate for endothelial lineage using a heterokaryon model to screen for genes regulating EC development. In this model, an array of EC function-associated genes are sequentially activated in the ESC nuclei of chimeric heterokaryons generated by fusing human ECs with mouse ESCs. The genes upregulated in this model system are often determinants of EC fate or EC identity maintenance. Angiogenesis is an EC function that generates microvasculature sprouting from preexisting vasculature. We find

that TBX20 plays a role in angiogenesis but not in vasculogenesis, the formation of major conduits during development. Since vasculogenesis requires de novo generation of angioblasts, it is unlikely that TBX20 plays a role in EC lineage establishment. Angiogenesis requires EC migration and proliferation, and interestingly, Tbx20 selectively controls EC migration but not proliferation. During development, the VEGFR2 signaling pathway is a major regulator of angiogenesis that induces both EC migration and proliferation. VEGF triggers many downstream signaling cascades (including PI3K-Akt[49], PLC-γ-ERK1/2[50], SRC-Small GTPase[51], p38[52]) that are involved in EC migration and/or proliferation[53]. We will investigate the particular effector(s) of VEGFR2 signaling pathway[53] responsible for TBX20-regulated angiogenesis in future studies. In our preliminary studies, we found that in the *in vitro* scratch assay, which initiates cell migration, TBX20 expression was increased (data not shown), it will be interesting to determine if TBX20 expression is enriched in tip cells, the cell type that spearheads cell migration during angiogenesis.

TBX20-PROK2-PROKR1 signaling in the relay of VEGF activity: a proangiogenic capacitor

Our initial studies suggest that Tbx20 regulates angiogenesis. Taking advantage of Tbx20 as a transcription factor, we performed unbiased qRT-PCR array for angiogenic genes to identify the Tbx20 downstream target(s). We found that Prok2 was dramatically downregulated in response to TBX20 knockdown. Our subsequent in study in animals and *in vitro* validated that TBX20 loss- and gain-of-function decreased and increased PROK2 expression, respectively. FGF1 and FGFR3 are markedly reduced in TBX20-deficient ECs, but forced expression of these genes could not correct disrupted angiogenesis in Tbx20 knockdown animals. Thus, our data suggest that Prok2 is a direct downstream target of TBX20, and that its activity is not dependent upon FGF. Importantly, administration of PROK2 enhanced angiogenesis and functional recovery from hindlimb ischemia, suggesting that PROK2 can be a potential therapeutic target. PROK2 signaling controls endothelial migration and angiogenesis preferentially through PROKR1, but not PROKR2. PROKR1 KD impairs proper activation and phosphorylation of ERK1/2 and Akt. However, a survey of available TBX20 ChIP data failed to reveal TBX20 binding on PROK2 proximal promoter. Several reasons may account for this: 1. The quality of the ChIP data may not be optimal enough to allow for a high-resolution analysis of TBX20 binding to the Prok2 promoter region. 2. There may be some enhancer region(s) that is far away from the actual gene body regulating its expression. 3. Tbx20 may regulate Prok2 expression epigenetically or through a non-coding RNA. The detailed mechanism of action by which TBX20 regulates PROK2-PROKR1 signaling in angiogenesis warrants further investigation.

PROK2, known as a member of endocrine gland-derived VEGF family, is expressed in the endocrine tissues. In the testis where the turnover of ECs is high, PROK2 and its receptor PROKR1 are highly expressed, which may help maintain vascular integrity and density in the adult[54]. During early pregnancy, PROKR1 is expressed in the fetal ECs to support gestation. Our study identified the role of this pathway in developmental and pathological angiogenesis. Although several GPCR ligands such as S1P or Apelin regulate angiogenesis[55–57], they usually employ a paracrine mechanism, i.e. other cells that secrete the ligands acting on ECs. We elucidated a novel autocrine GPCR signaling cascade in

which EC-derived GPCR ligand PROK2 controls endothelial migration and angiogenesis. Angiogenesis is required for embryogenesis and tissue remodeling/repair following ischemia. Because partial VEGF loss- or gain-of-function causes embryonic lethality[58–60], it is essential to evolve multiple layers of control mechanisms to ensure proper VEGF signaling, e.g. an alternative pathway to sustain the proangiogenic effect. We speculate that this TBX20-PROK2-PROKR1 pathway may thereby function as a "biological capacitor" to relay and prolong the angiogenesis-promoting effect of VEGF. To conclude, our studies highlight a previously unappreciated mechanism for angiogenesis in which VEGF-stimulated TBX20 activates PROK2-PROKR1 signaling. This pathway might be therapeutically targeted to treat diseases associated with dysregulated angiogenesis.

Supplementary Material

Refer to Web version on PubMed Central for supplementary material.

Acknowledgments

Sources of funding

This work is supported by grants from the National Institutes of Health (U01 HL100397), National Eye Institute (R01 HL02060901) and the Cancer Prevention and Research Institute (RP150611) to J.P.C, and by grants (HL114734, HL132155, and 16BGIA27790081) to L.F. S.M is supported by American Heart Association Scientist Development Grant (17SDG33660090). X.Y is supported by postdoctoral fellowship from the American Heart Association (17POST33410671).

References

1. Meins M, Henderson DJ, Bhattacharya SS, Sowden JC. Characterization of the human TBX20 gene, a new member of the T-Box gene family closely related to the Drosophila H15 gene. Genomics. 2000; 67:317–32. [PubMed: 10936053]
2. Griffin KJ, Stoller J, Gibson M, Chen S, Yelon D, Stainier DY, Kimelman D. A conserved role for H15-related T-box transcription factors in zebrafish and Drosophila heart formation. Dev Biol. 2000; 218:235–47. [PubMed: 10656766]
3. Ahn D-gRuvinsky I, Oates AC, Silver LM, Ho RK. tbx20, a new vertebrate T-box gene expressed in the cranial motor neurons and developing cardiovascular structures in zebrafish. Mech Dev. 2000; 95:253–258. [PubMed: 10906473]
4. Szeto DP, Griffin KJ, Kimelman D. HrT is required for cardiovascular development in zebrafish. Development. 2002; 129:5093–5101. [PubMed: 12397116]
5. Stennard FA, Harvey RP. T-box transcription factors and their roles in regulatory hierarchies in the developing heart. Development. 2005; 132:4897–910. [PubMed: 16258075]
6. Cai CL, Zhou W, Yang L, Bu L, Qyang Y, Zhang X, Li X, Rosenfeld MG, Chen J, Evans S. T-box genes coordinate regional rates of proliferation and regional specification during cardiogenesis. Development. 2005; 132:2475–87. [PubMed: 15843407]
7. Singh MK, Christoffels VM, Dias JM, Trowe MO, Petry M, Schuster-Gossler K, Burger A, Ericson J, Kispert A. Tbx20 is essential for cardiac chamber differentiation and repression of Tbx2. Development. 2005; 132:2697–707. [PubMed: 15901664]
8. Kirk EP, Sunde M, Costa MW, Rankin SA, Wolstein O, Castro ML, Butler TL, Hyun C, Guo G, Otway R, Mackay JP, Waddell LB, Cole AD, Hayward C, Keogh A, Macdonald P, Griffiths L, Fatkin D, Sholler GF, Zorn AM, Feneley MP, Winlaw DS, Harvey RP. Mutations in cardiac T-box factor gene TBX20 are associated with diverse cardiac pathologies, including defects of septation and valvulogenesis and cardiomyopathy. Am J Hum Genet. 2007; 81:280–91. [PubMed: 17668378]
9. Shelton EL, Yutzey KE. Tbx20 regulation of endocardial cushion cell proliferation and extracellular matrix gene expression. Dev Biol. 2007; 302:376–88. [PubMed: 17064679]

10. Boogerd CJ, Aneas I, Sakabe N, Dirschinger RJ, Cheng QJ, Zhou B, Chen J, Nobrega MA, Evans SM. Probing chromatin landscape reveals roles of endocardial TBX20 in septation. J Clin Invest. 2016; 126:3023–35. [PubMed: 27348591]
11. Cai X, Zhang W, Hu J, Zhang L, Sultana N, Wu B, Cai W, Zhou B, Cai CL. Tbx20 acts upstream of Wnt signaling to regulate endocardial cushion formation and valve remodeling during mouse cardiogenesis. Development. 2013; 140:3176–87. [PubMed: 23824573]
12. Takeuchi JK, Mileikovskaia M, Koshiba-Takeuchi K, Heidt AB, Mori AD, Arruda EP, Gertsenstein M, Georges R, Davidson L, Mo R, Hui CC, Henkelman RM, Nemer M, Black BL, Nagy A, Bruneau BG. Tbx20 dose-dependently regulates transcription factor networks required for mouse heart and motoneuron development. Development. 2005; 132:2463–74. [PubMed: 15843409]
13. Xiang FL, Guo M, Yutzey KE. Overexpression of Tbx20 in Adult Cardiomyocytes Promotes Proliferation and Improves Cardiac Function After Myocardial Infarction. Circulation. 2016; 133:1081–92. [PubMed: 26841808]
14. Chakraborty S, Sengupta A, Yutzey KE. Tbx20 promotes cardiomyocyte proliferation and persistence of fetal characteristics in adult mouse hearts. J Mol Cell Cardiol. 2013; 62:203–13. [PubMed: 23751911]
15. Shen T, Aneas I, Sakabe N, Dirschinger RJ, Wang G, Smemo S, Westlund JM, Cheng H, Dalton N, Gu Y, Boogerd CJ, Cai CL, Peterson K, Chen J, Nobrega MA, Evans SM. Tbx20 regulates a genetic program essential to adult mouse cardiomyocyte function. J Clin Invest. 2011; 121:4640–54. [PubMed: 22080862]
16. Shen T, Zhu Y, Patel J, Ruan Y, Chen B, Zhao G, Cao Y, Pang J, Guo H, Li H, Man Y, Wang S, Li J. T-box20 suppresses oxidized low-density lipoprotein-induced human vascular endothelial cell injury by upregulation of PPAR-gamma. Cell Physiol Biochem. 2013; 32:1137–50. [PubMed: 24247152]
17. Bhutani N, Brady JJ, Damian M, Sacco A, Corbel SY, Blau HM. Reprogramming towards pluripotency requires AID-dependent DNA demethylation. Nature. 2010; 463:1042–7. [PubMed: 20027182]
18. Wong WT, Matrone G, Tian X, Tomoiaga SA, Au KF, Meng S, Yamazoe S, Sieveking D, Chen K, Burns DM, Chen JK, Blau HM, Cooke JP. Discovery of novel determinants of endothelial lineage using chimeric heterokaryons. Elife. 2017; 6:e23588.doi: 10.7554/eLife.23588 [PubMed: 28323620]
19. Fang L, Choi SH, Baek JS, Liu C, Almazan F, Ulrich F, Wiesner P, Taleb A, Deer E, Pattison J, Torres-Vazquez J, Li AC, Miller YI. Control of angiogenesis by AIBP-mediated cholesterol efflux. Nature. 2013; 498:118–22. [PubMed: 23719382]
20. Gu Q, Yang X, Lin L, Li S, Li Q, Zhong S, Peng J, Cui Z. Genetic ablation of solute carrier family 7a3a leads to hepatic steatosis in zebrafish during fasting. Hepatology. 2014; 60:1929–1941. [PubMed: 25130427]
21. Mao R, Meng S, Gu Q, Araujo-Gutierrez R, Kumar S, Yan Q, Almazan F, Youker KA, Fu Y, Pownall HJ, Cooke JP, Miller YI, Fang L. AIBP Limits Angiogenesis Through gamma-Secretase-Mediated Upregulation of Notch Signaling. Circ Res. 2017
22. Sayed N, Wong WT, Ospino F, Meng S, Lee J, Jha A, Dexheimer P, Aronow BJ, Cooke JP. Transdifferentiation of human fibroblasts to endothelial cells: role of innate immunity. Circulation. 2015; 131:300–9. [PubMed: 25359165]
23. Huang NF, Niiyama H, Peter C, De A, Natkunam Y, Fleissner F, Li Z, Rollins MD, Wu JC, Gambhir SS, Cooke JP. Embryonic stem cell-derived endothelial cells engraft into the ischemic hindlimb and restore perfusion. Arterioscler Thromb Vasc Biol. 2010; 30:984–91. [PubMed: 20167654]
24. Brenes RA, Jadlowiec CC, Bear M, Hashim P, Protack CD, Li X, Lv W, Collins MJ, Dardik A. Toward a mouse model of hind limb ischemia to test therapeutic angiogenesis. J Vasc Surg. 2012; 56:1669–79. discussion 1679. [PubMed: 22836102]
25. Jao LE, Wente SR, Chen WB. Efficient multiplex biallelic zebrafish genome editing using a CRISPR nuclease system. Proc Natl Acad Sci U S A. 2013; 110:13904–13909. [PubMed: 23918387]

26. Meng S, Zhou G, Gu Q, Chanda PK, Ospino F, Cooke JP. Transdifferentiation Requires iNOS Activation: Role of RING1A S-Nitrosylation. Circ Res. 2016; 119:e129–e138. [PubMed: 27623813]
27. Yang X, Gu Q, Lin L, Li S, Zhong S, Li Q, Cui Z. Nucleoporin 62-like protein activates canonical Wnt signaling through facilitating the nuclear import of β-catenin in zebrafish. Mol Cell Biol. 2015; 35:1110–1124. [PubMed: 25605329]
28. Zhai G, Gu Q, He J, Lou Q, Chen X, Jin X, Bi E, Yin Z. Sept6 is required for ciliogenesis in Kupffer's vesicle, the pronephros, and the neural tube during early embryonic development. Mol Cell Biol. 2014; 34:1310–1321. [PubMed: 24469395]
29. Nicoli S, Presta M. The zebrafish/tumor xenograft angiogenesis assay. Nat Protoc. 2007; 2:2918–23. [PubMed: 18007628]
30. Serbedzija GN, Flynn E, Willett CE. Zebrafish angiogenesis: a new model for drug screening. Angiogenesis. 1999; 3:353–9. [PubMed: 14517415]
31. Lawson ND, Weinstein BM. In vivo imaging of embryonic vascular development using transgenic zebrafish. Dev Biol. 2002; 248:307–318. [PubMed: 12167406]
32. Isogai S, Lawson ND, Torrealday S, Horiguchi M, Weinstein BM. Angiogenic network formation in the developing vertebrate trunk. Development. 2003; 130:5281–5290. [PubMed: 12954720]
33. Hen G, Nicenboim J, Mayseless O, Asaf L, Shin M, Busolin G, Hofi R, Almog G, Tiso N, Lawson ND, Yaniv K. Venous-derived angioblasts generate organ-specific vessels during zebrafish embryonic development. Development. 2015; 142:4266–78. [PubMed: 26525671]
34. Kok FO, Shin M, Ni CW, Gupta A, Grosse AS, van Impel A, Kirchmaier BC, Peterson-Maduro J, Kourkoulis G, Male I, DeSantis DF, Sheppard-Tindell S, Ebarasi L, Betsholtz C, Schulte-Merker S, Wolfe SA, Lawson ND. Reverse genetic screening reveals poor correlation between morpholino-induced and mutant phenotypes in zebrafish. Dev Cell. 2015; 32:97–108. [PubMed: 25533206]
35. Macindoe I, Glockner L, Vukasin P, Stennard FA, Costa MW, Harvey RP, Mackay JP, Sunde M. Conformational stability and DNA binding specificity of the cardiac T-box transcription factor Tbx20. J Mol Biol. 2009; 389:606–18. [PubMed: 19414016]
36. Rossi A, Kontarakis Z, Gerri C, Nolte H, Hölper S, Krüger M, Stainier DY. Genetic compensation induced by deleterious mutations but not gene knockdowns. Nature. 2015; 524:230–233. [PubMed: 26168398]
37. Yelon D, Horne SA, Stainier DY. Restricted expression of cardiac myosin genes reveals regulated aspects of heart tube assembly in zebrafish. Dev Biol. 1999; 214:23–37. [PubMed: 10491254]
38. Kurebayashi H, Goi T, Shimada M, Tagai N, Naruse T, Nakazawa T, Kimura Y, Hirono Y, Yamaguchi A. Prokineticin 2 (PROK2) is an important factor for angiogenesis in colorectal cancer. Oncotarget. 2015; 6:26242–51. [PubMed: 26317645]
39. Curtis VF, Wang H, Yang P, McLendon RE, Li X, Zhou QY, Wang XF. A PK2/Bv8/PROK2 antagonist suppresses tumorigenic processes by inhibiting angiogenesis in glioma and blocking myeloid cell infiltration in pancreatic cancer. PLoS One. 2013; 8:e54916. [PubMed: 23372791]
40. Cheng MY, Bullock CM, Li C, Lee AG, Bermak JC, Belluzzi J, Weaver DR, Leslie FM, Zhou QY. Prokineticin 2 transmits the behavioural circadian rhythm of the suprachiasmatic nucleus. Nature. 2002; 417:405–10. [PubMed: 12024206]
41. Ng KL, Li JD, Cheng MY, Leslie FM, Lee AG, Zhou QY. Dependence of olfactory bulb neurogenesis on prokineticin 2 signaling. Science. 2005; 308:1923–7. [PubMed: 15976302]
42. Pitteloud N, Zhang C, Pignatelli D, Li JD, Raivio T, Cole LW, Plummer L, Jacobson-Dickman EE, Mellon PL, Zhou QY, Crowley WF Jr. Loss-of-function mutation in the prokineticin 2 gene causes Kallmann syndrome and normosmic idiopathic hypogonadotropic hypogonadism. Proc Natl Acad Sci U S A. 2007; 104:17447–52. [PubMed: 17959774]
43. Ayari B, El Hachimi KH, Yanicostas C, Landoulsi A, Soussi-Yanicostas N. Prokineticin 2 Expression Is Associated with Neural Repair of Injured Adult Zebrafish Telencephalon. J Neurotrauma. 2010; 27:959–972. [PubMed: 20102264]
44. Chen J, Kuei C, Sutton S, Wilson S, Yu J, Kamme F, Mazur C, Lovenberg T, Liu C. Identification and pharmacological characterization of prokineticin 2 beta as a selective ligand for prokineticin receptor 1. Mol Pharmacol. 2005; 67:2070–6. [PubMed: 15772293]

45. Dode C, Teixeira L, Levilliers J, Fouveaut C, Bouchard P, Kottler ML, Lespinasse J, Lienhardt-Roussie A, Mathieu M, Moerman A, Morgan G, Murat A, Toublanc JE, Wolczynski S, Delpech M, Petit C, Young J, Hardelin JP. Kallmann syndrome: mutations in the genes encoding prokineticin-2 and prokineticin receptor-2. PLoS Genet. 2006; 2:e175. [PubMed: 17054399]
46. Guilini C, Urayama K, Turkeri G, Dedeoglu DB, Kurose H, Messaddeq N, Nebigil CG. Divergent roles of prokineticin receptors in the endothelial cells: angiogenesis and fenestration. Am J Physiol Heart Circ Physiol. 2010; 298:H844–52. [PubMed: 20023120]
47. Urayama K, Guilini C, Turkeri G, Takir S, Kurose H, Messaddeq N, Dierich A, Nebigil CG. Prokineticin receptor-1 induces neovascularization and epicardial-derived progenitor cell differentiation. Arterioscler Thromb Vasc Biol. 2008; 28:841–9. [PubMed: 18421008]
48. Urayama K, Dedeoglu DB, Guilini C, Frantz S, Ertl G, Messaddeq N, Nebigil CG. Transgenic myocardial overexpression of prokineticin receptor-2 (GPR73b) induces hypertrophy and capillary vessel leakage. Cardiovasc Res. 2009; 81:28–37. [PubMed: 18806277]
49. Karar J, Maity A. PI3K/AKT/mTOR Pathway in Angiogenesis. Front Mol Neurosci. 2011; 4:51. [PubMed: 22144946]
50. Lawson ND, Mugford JW, Diamond BA, Weinstein BM. phospholipase C gamma-1 is required downstream of vascular endothelial growth factor during arterial development. Genes Dev. 2003; 17:1346–51. [PubMed: 12782653]
51. Chrzanowska-Wodnicka M. Regulation of angiogenesis by a small GTPase Rap1. Vascul Pharmacol. 2010; 53:1–10. [PubMed: 20302970]
52. Yu J, Bian D, Mahanivong C, Cheng RK, Zhou W, Huang S. p38 Mitogen-activated protein kinase regulation of endothelial cell migration depends on urokinase plasminogen activator expression. J Biol Chem. 2004; 279:50446–54. [PubMed: 15371454]
53. Simons M, Gordon E, Claesson-Welsh L. Mechanisms and regulation of endothelial VEGF receptor signalling. Nat Rev Mol Cell Biol. 2016; 17:611–25. [PubMed: 27461391]
54. LeCouter J, Lin R, Tejada M, Frantz G, Peale F, Hillan KJ, Ferrara N. The endocrine-gland-derived VEGF homologue Bv8 promotes angiogenesis in the testis: Localization of Bv8 receptors to endothelial cells. Proc Natl Acad Sci U S A. 2003; 100:2685–90. [PubMed: 12604792]
55. Cox CM, D'Agostino SL, Miller MK, Heimark RL, Krieg PA. Apelin, the ligand for the endothelial G-protein-coupled receptor, APJ, is a potent angiogenic factor required for normal vascular development of the frog embryo. Dev Biol. 2006; 296:177–189. [PubMed: 16750822]
56. Yanagida K, Hla T. Vascular and Immunobiology of the Circulatory Sphingosine 1-Phosphate Gradient. Annu Rev Physiol. 2017; 79:67–91. [PubMed: 27813829]
57. Kang YJ, Kim JM, Anderson JP, Wu JX, Gleim SR, Kundu RK, McLean DL, Kim JD, Park H, Jin SW, Hwa J, Quertermous T, Chun HJ. Apelin-APJ Signaling Is a Critical Regulator of Endothelial MEF2 Activation in Cardiovascular Development. Circ Res. 2013; 113:22–31. [PubMed: 23603510]
58. Miquerol L, Langille BL, Nagy A. Embryonic development is disrupted by modest increases in vascular endothelial growth factor gene expression. Development. 2000; 127:3941–6. [PubMed: 10952892]
59. Carmeliet P, Ferreira V, Breier G, Pollefeyt S, Kieckens L, Gertsenstein M, Fahrig M, Vandenhoeck A, Harpal K, Eberhardt C, Declercq C, Pawling J, Moons L, Collen D, Risau W, Nagy A. Abnormal blood vessel development and lethality in embryos lacking a single VEGF allele. Nature. 1996; 380:435–9. [PubMed: 8602241]
60. Ferrara N, Carver-Moore K, Chen H, Dowd M, Lu L, O'Shea KS, Powell-Braxton L, Hillan KJ, Moore MW. Heterozygous embryonic lethality induced by targeted inactivation of the VEGF gene. Nature. 1996; 380:439–42. [PubMed: 8602242]

Clinical Perspective

What's new?

- We report a novel TBX20-choreographed signaling pathway that functions as a proangiogenic capacitor to regulate developmental and pathological angiogenesis.
- In this signaling pathway, with VEGF stimulation, the transcription factor TBX20 upregulates PROK2, which is secreted from endothelial cells (ECs), engages its receptor PROKR1, and thereby promotes angiogenesis in an autocrine manner.
- This signaling pathway (TBX20-PROK2-PROKR1) is highly conserved as it functions in zebrafish vascular development, and the angiogenic response to ischemia in a mouse model of peripheral arterial disease (PAD).
- Our study indicates the selective role of TBX20 in endothelial migration but not proliferation.

What are the clinical implications?

- Stimulating this pathway may facilitate therapeutic angiogenesis in patients with ischemic syndromes such as PAD.
- Treatment with recombinant PROK2, the critical effector of TBX20, improves blood perfusion and functional recovery in the mouse PAD model.
- Mutations in *TBX20*, *PROK2*, or *PROKR1* gene precipitate cardiovascular or neuronal diseases in humans.
- Our data highlight the therapeutic potential of PROK2 in augmenting functional angiogenesis for diseases associated with dysregulated angiogenesis.

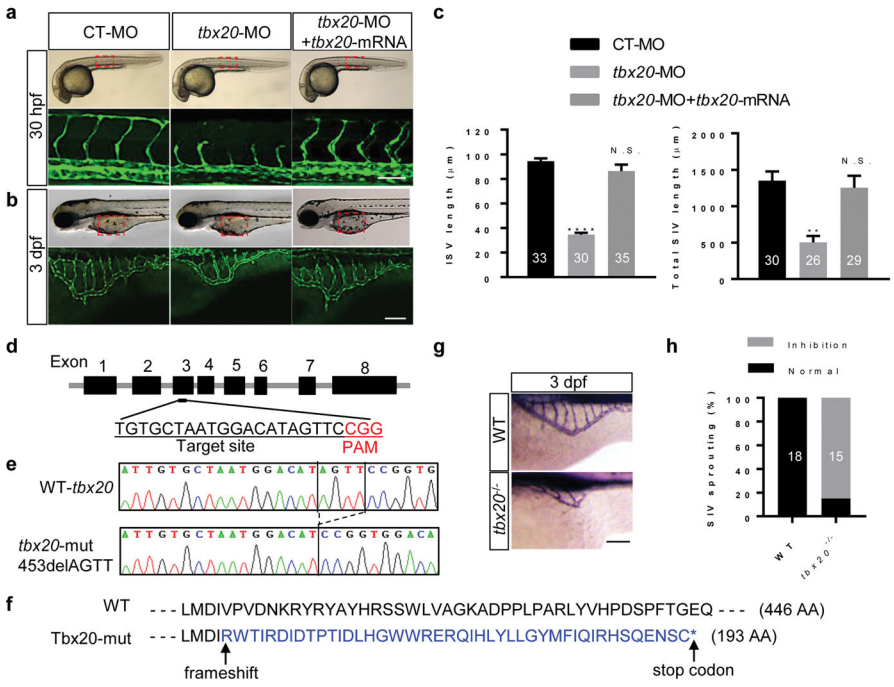

Figure 1. *Tbx20* is essential for developmental angiogenesis but not vasculogenesis

a & **b,** Bright-field images showing the gross morphology of 30 hpf (a, upper panel) or 3 dpf (**b,** upper panel) *Tg(fli1:EGFP)*^{y1} zebrafish embryos injected with CT-MO, *tbx20*-MO, or the combination of *tbx20*-MO and *tbx20* mRNA. The boxed regions (red) indicate confocal imaging locations. Morphology of ISVs (boxed region) in 30 hpf (**a,** lower panel) or SIVs (boxed region) in 3 dpf (**b**, lower panel) embryos. **c**, Quantification of the ISV length in a (left) or SIV length in **b** (right). **d**. Diagram showing the position and DNA sequence (underline) of the CRISRP/Cas9 target site of zebrafish *tbx20* gene locus. PAM sequence (CGG) is shown in red. **e**. Sanger sequencing results revealed a 4-bp genomic DNA fragment deletion from the target site in *tbx20* mutants. **f**. An alignment of the protein sequences encoded by WT Tbx20 (446 AA) and Tbx20 mutant (193 AA). A 4-bp deletion caused frameshift of open reading frame leading to a premature stop codon (marked as *). **g**. Representative alkaline phosphatase staining of SIVs in WT animals or *tbx20* mutants at 3 dpf. **h**. Quantification of WT animals or *tbx20* mutants showing normal or inhibited SIV sprouting in **g**. Scale bar: **a**, 100 μm; **b** & **g**, 60 μm. All data are presented as mean ± S.E.M; numbers of animals analyzed are indicated in the bars of c & h. N.S., not significant. **p≤ 0.01, ****p≤ 0.0001, compared with CT-MO group.

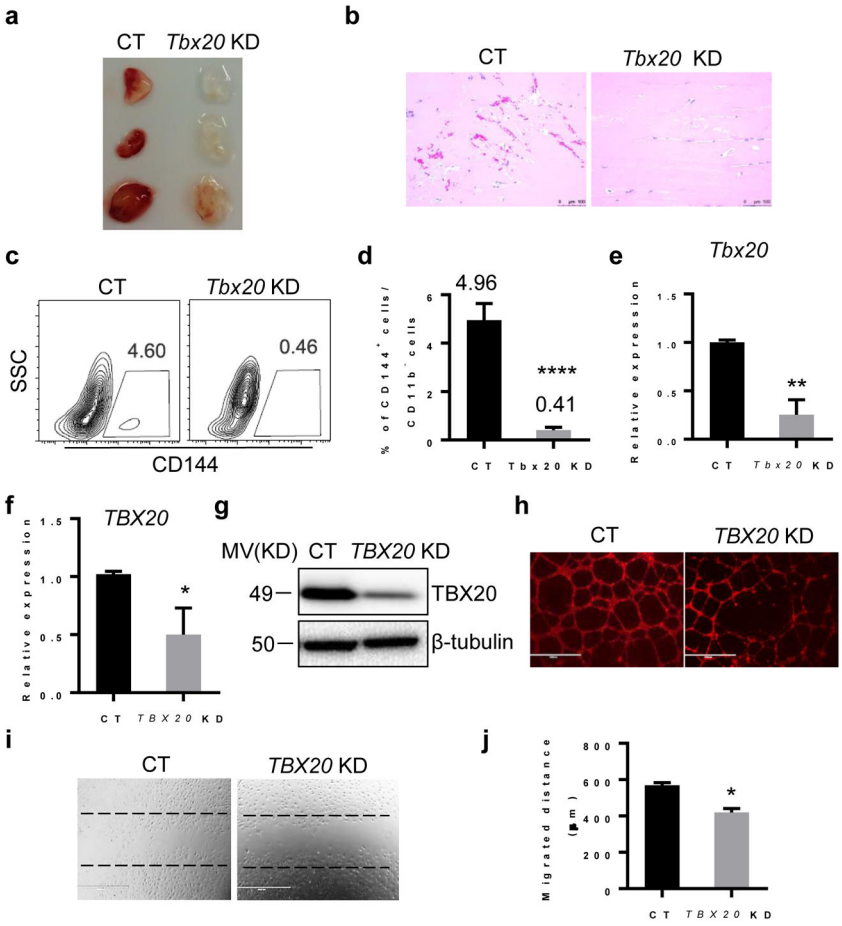

Figure 2. TBX20 modulates adult angiogenesis and endothelial migration

a. Bright field image of VEGF-induced angiogenesis in matrigel plugs that were premixed with CT or *Tbx20* siRNA (*Tbx20* KD). **b**. Representative images of HE staining of matrigel plugs with the indicated treatment. **c**. FACS analysis of $CD144^{+}$ cells in $CD11b^{-}$ population in digested matrigel plugs. **d**. Quantification of **c. e**. Quantitative RT-PCR analysis of *Tbx20* gene expression in matrigel plugs retrieved from mice. Quantitative RT-PCR examination of *TBX20* mRNA (**f**) and western blot analysis of TBX20 protein (**g**) in CT or *TBX20* KD HUVECs. **h**. Representative images of *in vitro* tube formation of CT or *TBX20* KD HUVECs. **i**. Representative images of cell migration after scratch. **j**. Quantification of cell migration in **i**. Scale bar: 100 μm. All data are expressed as mean ± S.E.M; n=3. *p≤ 0.05, **p≤ 0.01, ****p≤ 0.0001 vs CT.

a

Gene	Fold Change	Gene	Fold Change
PROK2	-12.4	IFNG	-4.8
COL4A3	-6.0	LECT1	-10.2
CXCL9	-4.4	LEP	-4.2
EGF	-4.1	MMP9	-4.9
FGF1	-14.1	PF4	-6.6
FGFR3	-8.8	BAI1	-6.5
HGF	-7.7	THBS2	-8.0
IFNA1	-5.0	TNF	-4.1

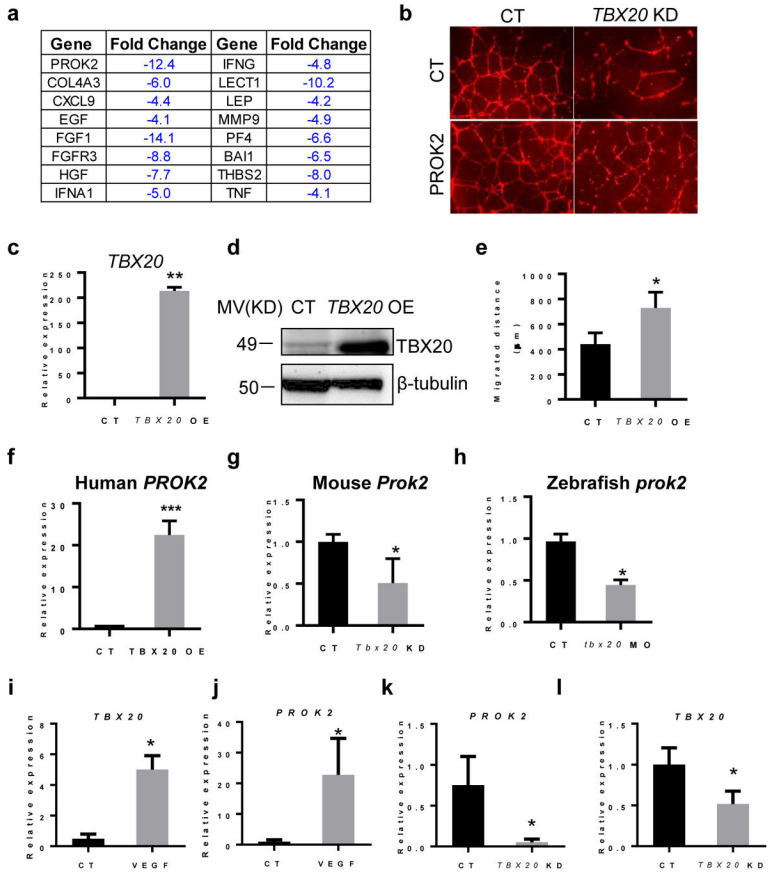

Figure 3. PROK2 mediates the effect of TBX20 on angiogenesis and cell migration

a. Lists of angiogenesis-related genes that were downregulated over two-fold in *TBX20* KD HUVECs compared with CT KD cells. **b.** Representative tube formation images of *TBX20* or CT KD HUVECs with or without recombinant PROK2 supplement. Quantitative RT-PCR analysis of TBX20 mRNA (**c)** and western blot assessment of TBX20 protein (**d**) in TBX20 OE HUVECs. **e.** Quantification of cell migration after scratch assay of CT and TBX20 OE HUVECs. **f.** *PROK2* gene expression in TBX20 OE or CT HUVECs. **g.** *Prok2* gene expression of the matrigel plugs implanted in mice. **h.** Trunk regions of zebrafish injected with CT or *tbx20* MO were dissected to analyze *prok2* gene expression. **i** & **j.** *TBX20* and *PROK2* gene expression in HUVECs stimulated with or without VEGFA165 50 ng/ml for 4 hr after scratch assay. **k** & **l.** *PROK2* and *TBX20* gene expression in stable TBX20 KD or CT HUVEC treated as in **i.** Scale bar: 100 μm. All data are expressed as mean ± S.E.M; n=3. *p≤ 0.05, **p≤ 0.01, ***p≤ 0.0001 vs CT.

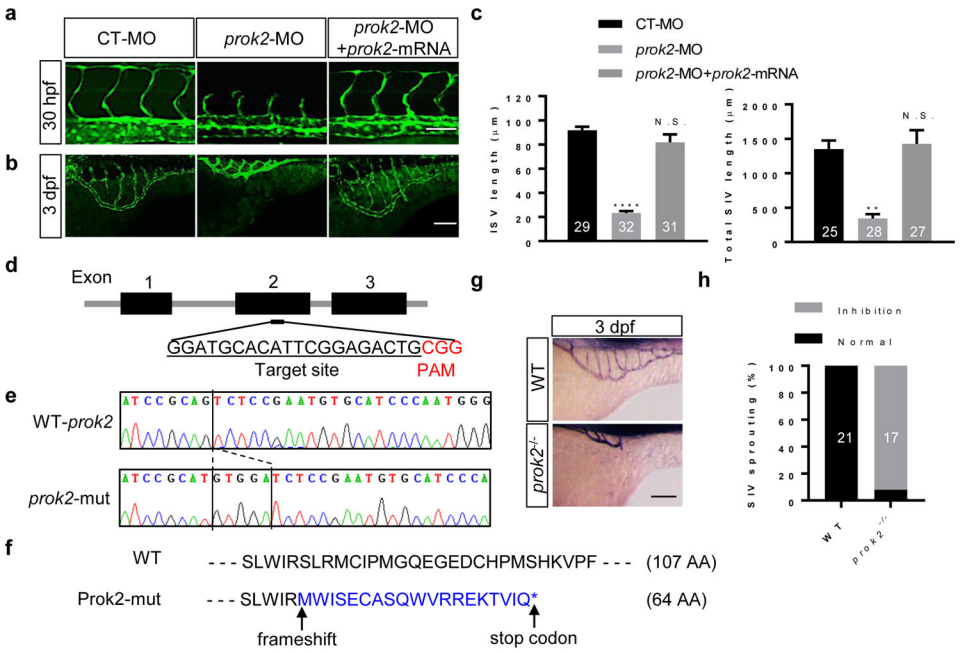

Figure 4. Effect of Prok2 deficiency on zebrafish developmental angiogenesis

a & **b**, *Tg(fli1:EGFP)*^{y1} zebrafish embryos were injected with CT-MO, *prok2*-MO, or the combination of *prok2*-MO and *prok2* mRNA, and ISV and SIV was imaged at 30 hpf (**a**) and at 3 dpf (**b**), respectively. **c**, Quantification of the ISV length in 30 hpf (left) or SIV length in 3 dpf animals (right) with the indicated treatment. **d**. Diagram showing the position and DNA sequence (underline) of the CRISRP/Cas9 target site of zebrafish *prok2* gene locus. PAM sequence (CGG) is shown in red. **e**. Sanger sequencing revealed a 5-bp genomic DNA fragment insertion from the target site in *prok2* mutants. **f**. An alignment of the protein sequences of WT Prok2 (107 AA) and Prok2 mutant protein (64 AA). A 5-bp insertion caused frameshift leading to a premature stop codon (marked as *). **g**. Alkaline phosphatase staining of SIVs in WT animals or *prok2* mutants at 3 dpf. **h**. Quantification of WT animals or *prok2* mutants showing normal or inhibited SIV sprouting in **g**. Scale bars, a, 100 μm; **b** & **g**, 60 μm. All data are expressed as mean ± S.E.M; numbers of animals analyzed are shown in the bars of **c** & **h**. N.S., not significant. **p≤ 0.01, ****p≤ 0.0001, compared with CT group.

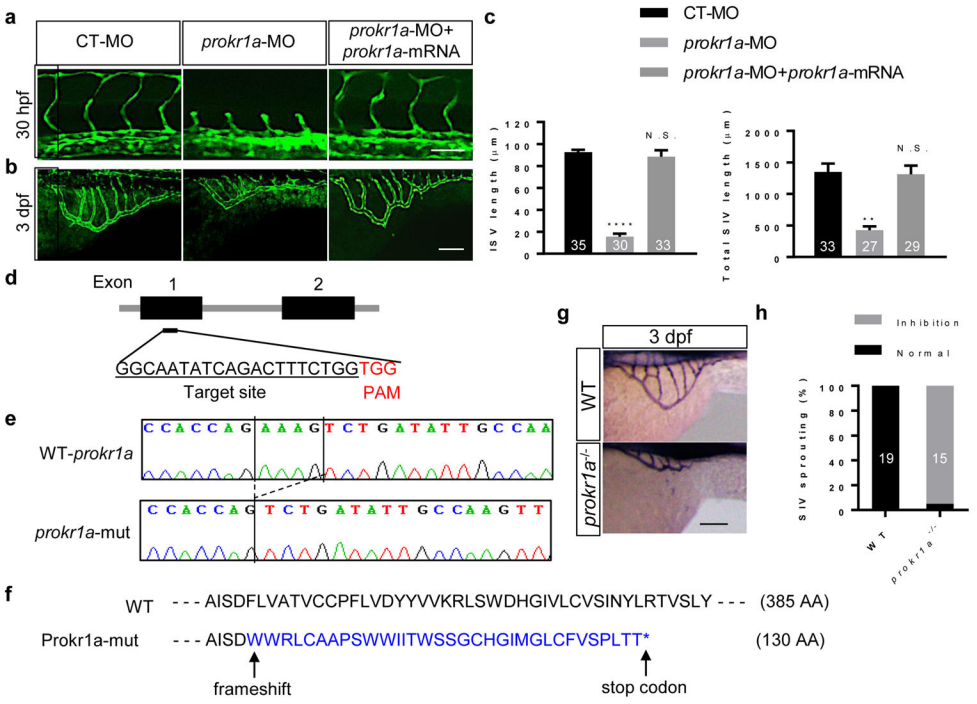

Figure 5. Effect of Prokr1a deficiency on zebrafish angiogenesis

a & **b**. *Tg(fli1:EGFP)*^{y1} zebrafish embryos were injected with CT-MO, *prokr1a*-MO, or the combination of *prokr1a*-MO and *prokr1a* mRNA, and ISV and SIV was imaged at 30 hpf (**a**) and at 3 dpf (**b**), respectively. **C**. Quantification of the ISV length in 30 hpf (left) or SIV length in 3 dpf embryos (right). **d**. Diagram showing the position and DNA sequence (underline) of the CRISRP/Cas9 target site of zebrafish *prokr1a* gene locus. PAM sequence (TGG) is shown in red. **e**. Sanger sequencing results revealed a 4-bp genomic DNA fragment deletion from the target site in *prokr1a* mutants. **f**. An alignment of the protein sequences of WT Prokr1a (385 AA) and Prokr1a mutant protein (130 AA). A 4-bp deletion caused frameshift leading to a premature stop codon (marked as *). g. Alkaline phosphatase staining of SIVs in WT animals or *prokr1a* mutants at 3 dpf. **h**. Quantification of WT animals or *prokr1a* mutants showing normal or inhibited SIV sprouting in g. Scale bar: **a**, 100 μm; b & g, 60 μm. All data are presented as mean ± S.E.M; numbers of animals analyzed are indicated in the bars of **c** & **h**. N.S., not significant. **p≤ 0.01, ****p≤ 0.0001, compared with CT-MO group.

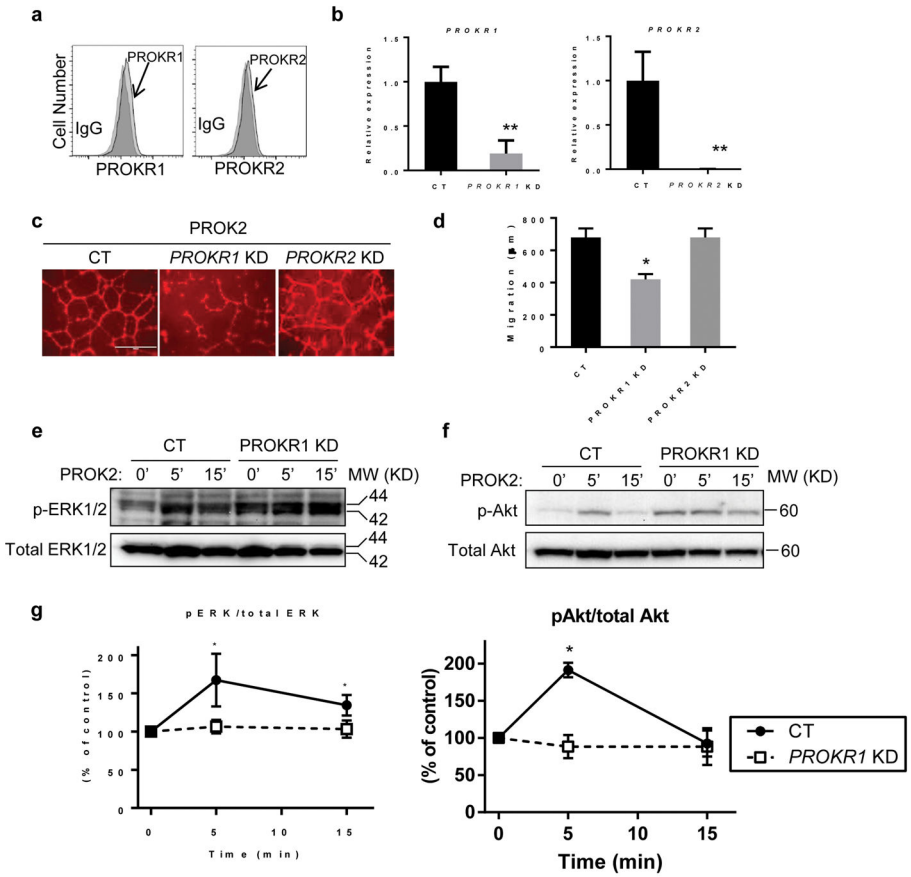

Figure 6. PROK2 controls angiogenesis and cell migration through PROKR1

a. FACS analysis of cell surface expression of PROKR1 and PROKR2 in HUVECs. **b**. *PROKR1* and *PROKR2* mRNA fold change of HUVECs treated with CT siRNA, PROKR1 siRNA, or PROKR2 siRNA. **c**. Representative image of tube formation of HUVECs transfected with CT siRNA, *PROKR1* siRNA, or *PROKR2* siRNA and stimulated with 60 ng/ml recombinant PROK2. **d**. Migration distance of HUVECs treated as in **c** and subjected to scratch assay. **e** & **f**. Western blot analysis of p-ERK1/2 and total ERK1/2 (**e**) or p-Akt and total Akt (**f**) in HUVECs transfected with CT siRNA or *PROKR1* siRNA and stimulated with recombinant PROK2. **g**. Quantitative data of **e** & **f**. The intensity of pERK1/2, total ERK1/2, pAkt, and total Akt immunoblotting signals was measured and normalized with baseline level at 0 min. Scale bar: 100 μm. All data are presented as mean ± S.E.M; n=3. *p≤ 0.05, **p≤ 0.01.

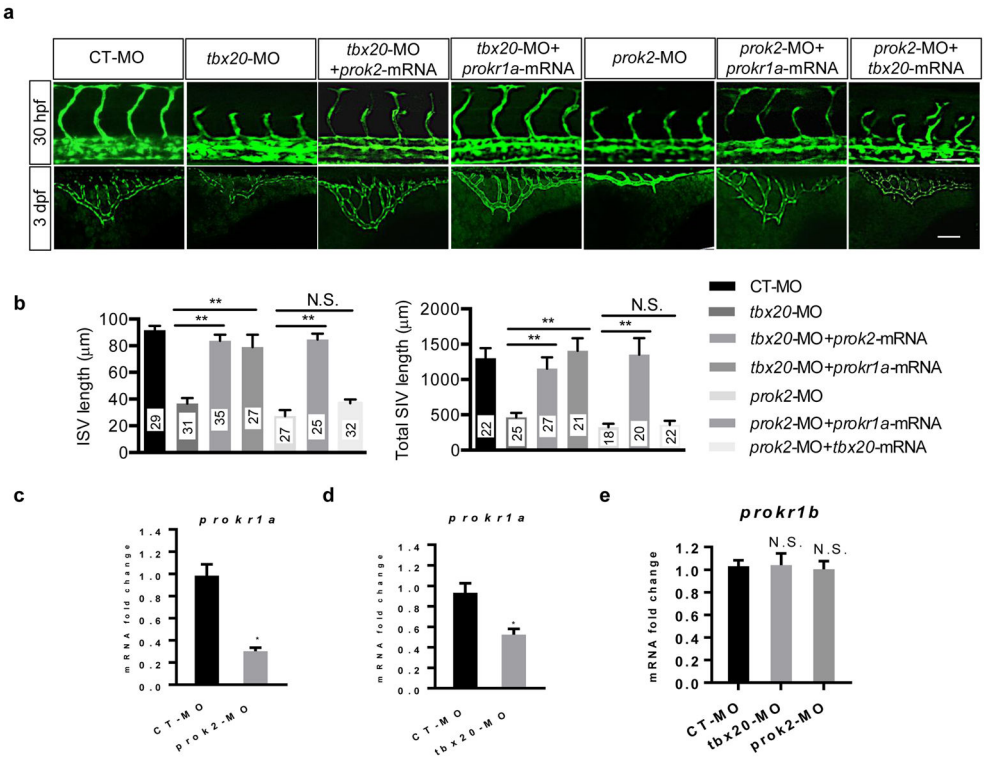

Figure 7. Prok2-Prokr1a is downstream of Tbx20 in controlling angiogenesis

a. Morphology of ISVs in 30 hpf (upper panel) or SIVs in 3 dpf (lower pannel) animals with the indicated treatment. **b**. Quantification of ISV length in 30 hpf (left) or SIV length in 3 dpf animals (right) from **a**. *prokr1a* gene expression in CT or *prok2* morphants (**c**) and in CT or *tbx20* morphants (**d**). **e**. *prokr1b* gene expression in CT, Tbx20, or Prok2 knockdown animals, 50 embryos were pooled in each group. Scale bar: a (upper),100 μm; a (lower), 60 μm. All data are presented as mean ± S.E.M; numbers of animals analyzed are indicated in the bars of **b**. N.S., not significant. *p≤ 0.05, **p≤ 0.01.

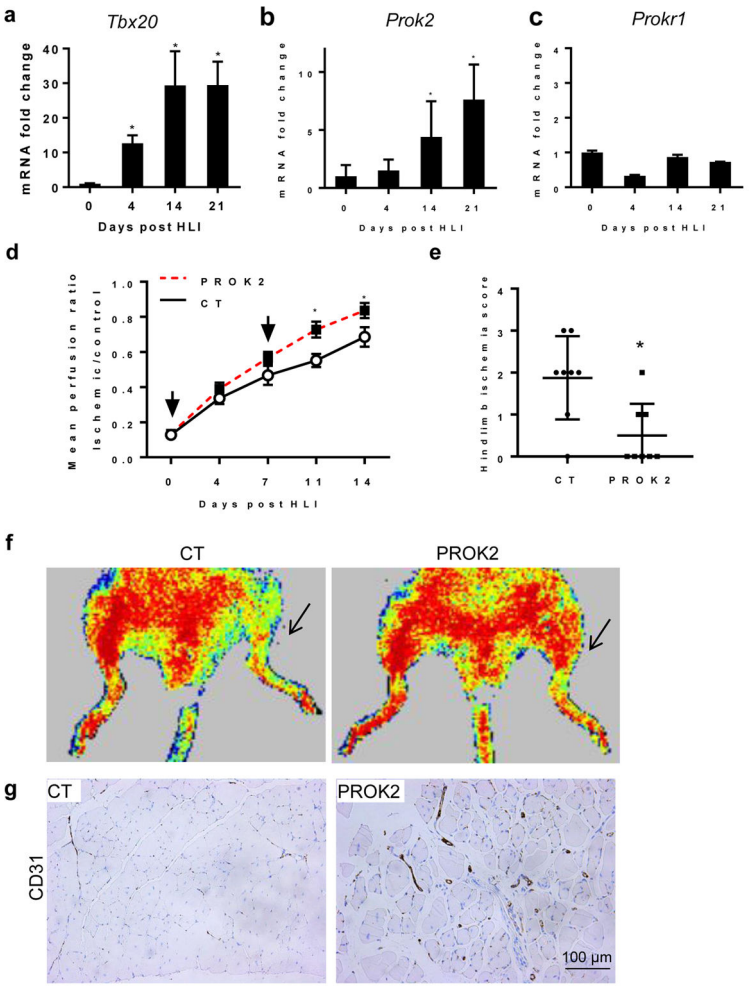

Figure 8. PROK2 enhances recovery from hindlimb ischemia

Ten months old mice were subjected to hindlimb ischemia, and recombinant PROK2 (0.1 μg/g body weight) or PBS was injected i.m. right after the surgery and at day 7 after surgery. Blood perfusion was monitored before, immediately after, and 4, 7, 11 and 14 days after the surgery. Limb muscles were dissected at day 14 for histological analysis. **a**–**c**. Gene expression of *Tbx20* (**a**), *Prok2* (**b**) and *Prokr1* (**c**) of limb muscles dissected at 0, 4, 14, and 21 days after surgery in CT group. **d**. Mean perfusion ratio of ischemic to un-operated limb at different time points after injury. **e**. Hindlimb ischemia score at day 14. **f**. Ultrasound imaging of blood perfusion in CT or PROK2-treated mice 14 days after ischemia. **g**. CD31 immunohistochemistry analysis of microvessels in the hindlimb muscle of CT or PROK2-treated animals. All data are presented as mean ± S.E.M; n=10 per group. *p≤ 0.05 compared to CT group.